Computational Studies of the Photophysics of Neutral and Zwitterionic Amino Acids in an Aqueous Environment: Tyrosine−$(H_2O)_2$ and Tryptophan−$(H_2O)_2$ Clusters

Andrzej L. Sobolewski,*,† Dorit Shemesh,‡ and Wolfgang Domcke‡

Institute of Physics, Polish Academy of Sciences, PL-02668 Warsaw, Poland, and Department of Chemistry, Technische Universität München, D-85747 Garching, Germany

Received: October 16, 2008; Revised Manuscript Received: December 1, 2008

Tyrosine−$(H_2O)_2$ and tryptophan−$(H_2O)_2$ clusters have been considered as models for the study of the photochemistry of neutral and zwitterionic tyrosine and tryptophan in an aqueous environment. It has been found that the detachment of neutral NH_3 in the S_1 state of the zwitterionic clusters leads to a low-lying conical intersection of the S_1 and S_0 energy surfaces. This conical intersection can provide the mechanism for efficient radiationless deactivation of the excited state back to the ground state or, alternatively, deamination (loss of ammonia). These results provide a mechanistic explanation of the efficient fluorescence quenching and the high quantum yield of ammonia in the UV photolysis of tyrosine and tryptophan in aqueous solution.

1. Introduction

Tryptophan (Trp) and tyrosine (Tyr) are the main UV-absorbing amino acids of proteins. Trp is known to be the photochemically most labile of the amino acids.[1−3] In addition, its fluorescence properties are particularly sensitive to the environment.[4,5] The mechanisms of the nonradiative decay and the photochemistry of Trp and Tyr have been the subject of extensive investigations and considerable controversy over several decades.[4−6]

It has long been known that UV irradiation of Trp (Tyr) in aqueous solution leads to tryptophyl (tyrosyl) radicals and hydrated electrons.[7−11] After the resolution of a dispute in the earlier literature, it seems to be established that this so-called photoionization of Tyr and Trp is a monophotonic process and that the threshold for photoionization coincides with the lowest $^1\pi\pi^*$ state of Trp or Tyr.[12−14] Because the chromophores indole (phenol) of Trp (Tyr) exhibit the same photoionization processes in aqueous solution, it has been concluded that the electron ejection occurs from these chromophores.[7,8]

Investigations of the photochemistry of size-selected clusters of indole and phenol with water and ammonia have revealed the existence of a hydrogen-transfer process from the chromophore to the solvent, which is driven by a photochemically reactive electronic state of $^1\pi\sigma^*$ character.[15−18] The H_3O or NH_4 hypervalent radicals formed in this photoinduced biradical dissociation process are the precursors of the solvated electron in the liquid phase.[19−21]

In the region of pH 4−8, where Trp and Tyr are expected to exist in their zwitterionic forms in aqueous solution, additional fluorescence quenching processes have been observed and tentatively interpreted as electron or proton transfer processes from the charged side groups to the chromophore or vice versa.[4,6,13,22−24] In addition, deamination (loss of ammonia) has been observed as one of the major photochemical channels of Trp and Tyr as well as of polypeptides involving Trp or Tyr.[1−6,25−27]

In the gas phase, the neutral covalent structures of Trp and Tyr are more stable than the zwitterions. The UV spectra of the former have been recorded with laser-induced fluorescence (LIF) spectroscopy in supersonic jets[28−32] or, more recently, in helium droplets.[33] Six (seven) low-lying conformers have been confirmed by resonantly enhanced two-photon ionization (R2PI) and UV hole-burning experiments for Tyr (Trp).[34−36] For the smallest amino acid glycine, ab initio calculations have shown that seven or eight water molecules are necessary to establish a zwitterionic global minimum.[37] Whereas R2PI spectra of Trp−water clusters have been obtained,[29,38,39] the existence of zwitterionic structures of Trp or Tyr in cold water clusters has not yet been confirmed.[40,41]

In the present investigation, we have explored the basic mechanisms of the photochemistry of the neutral and zwitterionic forms of Trp and Tyr in an aqueous microenvironment with computational methods. It is shown that the Tyr−$(H_2O)_2$ and Trp−$(H_2O)_2$ clusters possess, in addition to the global minimum of the neutral form, a (metastable) local minimum corresponding to a hydrated zwitterion. Starting from these geometries, the excited-state potential-energy surfaces and minimum-energy reaction paths have been explored with the CC2 method, which is a simplified and cost-effective variant of the CCSD method.[42,43] We have explored the reaction path for proton transfer from the neutral to the zwitterionic structure in the first excited state, as well as in the ground state. We show, furthermore, that charge transfer from the COO^- group toward the NH_3^+ group weakens the C_α−N bond to such an extent that a barrierless reaction path on the S_1 potential-energy surface leads to a conical intersection of the S_1 and S_0 surfaces. This conical intersection provides the mechanism for either efficient radiationless decay to the electronic ground state or the detachment of ammonia.

As mentioned above, eight or more water molecules may be necessary to render the zwitterionic structures of tryptophan−water or tyrosine−water clusters a global energy minimum. Calculations of excited-state energy surfaces and, in particular, extensive searches for excited-state minimum-energy reaction paths and conical intersections would be prohibitively expensive at present for large tryptophan−water or tyrosine−water clusters. The Tyr−$(H_2O)_2$ and Tyr−$(H_2O)_2$ clusters may serve, however,

* Author to whom correspondence should be addressed (e-mail sobola@ifpan.edu.pl).
† Polish Academy of Sciences.
‡ Technische Universität München.

10.1021/jp8091754 CCC: $40.75
Published on Web 12/19/2008

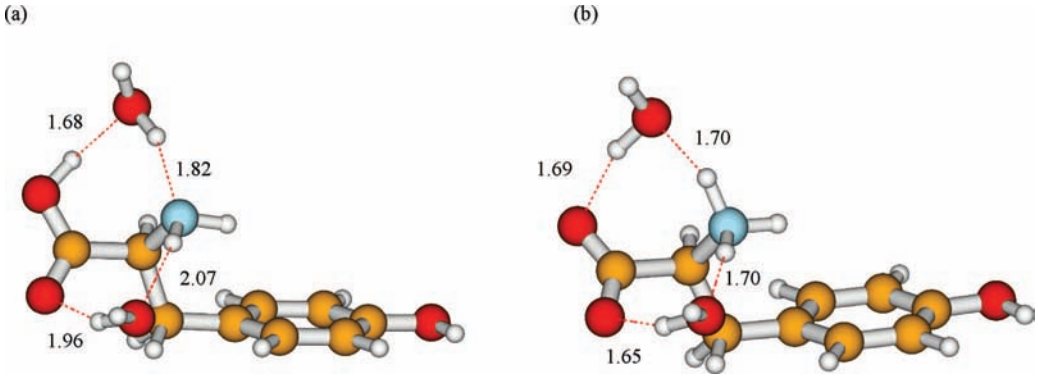

Figure 1. Ground-state equilibrium geometries of the neutral (a) and zwitterionic (b) forms of tyrosine$-(H_2O)_2$. Bond lengths are given in angstroms.

as useful model systems for the exploration of excited-state reaction mechanisms that are characteristic for hydrated zwitterionic aromatic amino acids. Preliminary knowledge of these mechanisms will certainly be helpful for the future exploration of these photochemical reaction processes in larger clusters. For the extrapolation of these results to the liquid phase, the first solvation shell of explicit water molecules should be complemented by a polarizable continuum model.

2. Methodology

The ground-state equilibrium geometries and reaction paths of the hydrogen-bonded Tyr$-(H_2O)_2$ complex (abbreviated Tyr$-W_2$ in the following) and the Trp$-(H_2O)_2$ complex (abbreviated Trp$-W_2$) have been determined with the second-order Møller−Plesset (MP2) method. Excitation energies and response properties have been calculated with the CC2 method,[42,43] which can be considered as the equivalent of MP2 for excited electronic states. The CC2 method has recently been applied and tested for various molecules. Schreiber et al.[44] and Fleig et al.[45] have benchmarked the accuracy of the CC2 method for organic molecules and nucleic acids. Georgieva et al. have performed a comparison of CC2 and TDDFT for 7-hydroxy-4-methylcoumarin.[46] Gregoire et al.[47] and Busker et al.[48] have tested CC2 in comparison with experimental data for protonated tryptophan and tyrosine as well as for 1-methylthymine with water. These applications have confirmed that the CC2 method is a reliable and efficient tool for the calculation of excitation energies and properties of biological molecules. It is not possible, at present, to use more sophisticated methods for the exploration of excited-state reaction paths due to the large size of the systems, their flexibility, and the lack of symmetry.

The equilibrium geometries and the reaction paths of the lowest excited singlet state of Tyr$-W_2$ and Trp$-W_2$ have been determined at the CC2 level, making use of CC2 analytic gradients.[49,50] To allow cost-effective explorations of the high-dimensional potential-energy surfaces, the standard split-valence double-ζ basis set of TURBOMOLE[51] with polarization functions on the heavy atoms (def-SV(P))[52] has been employed in these MP2 and CC2 geometry optimizations.

Two coordinate-driven minimum-energy reaction paths (relaxed scans) have been studied in the ground state and in the lowest excited singlet state of Tyr$-W_2$ and Trp$-W_2$. The first involves the transfer of the hydrogen atom of the carboxyl group to the amino group along the intermolecular hydrogen bonds of one of the water bridges. The reaction path leads from the neutral to the zwitterionic form of Tyr (Trp) in the Tyr$-W_2$ (Trp$-W_2$) cluster. The OH distance of the carboxyl group is chosen as the driving coordinate for the hydrogen-transfer reaction path. All other nuclear degrees of freedom have been optimized for a given value of the driving coordinate. The second reaction path studied in these systems is the detachment of the NH_3 group from the zwitterionic form of Tyr$-W_2$ and Trp$-W_2$. The $C_\alpha-N$ distance was chosen as the driving coordinate for this reaction path. This reaction path was found to lead to a low-lying conical intersection of the S_1 and S_0 potential energy surfaces. The relevant minima of the ground-state and excited-state energy surfaces were reoptimized at the MP2/cc-pVDZ and CC2/aug(N)-cc-pVDZ levels, respectively, where aug(N) indicates the addition of diffuse functions on the nitrogen of the amino group. It has been checked by test calculations with the fully augmented cc-pVDZ basis set that augmentation of the nitrogen atom of the amino group is sufficient for the present purposes. Single-point CC2 calculations were performed at the optimized minima of the ground state as well along the reaction paths on the S_0 and S_1 potential energy surfaces. In these calculations the aug(N)-cc-pVDZ basis set was used.

3. Results and Discussion

3.1. Structures. ***(i) Tyr$-W_2$.*** The equilibrium structures of the neutral and zwitterionic forms of the Tyr$-W_2$, obtained by unconstrained geometry optimization of the ground-state energy at the MP2/cc-pVDZ level, are shown in panels a and b, respectively, of Figure 1. The Cartesian geometry parameters of these structures are given in the Supporting Information. The structure of Figure 1a possibly is not the lowest energy neutral structure of the Tyr$-W_2$ cluster. The geometry was chosen such that it possesses the water bridges which are characteristic for the zwitterionic structures. The zwitterionic structure shown in Figure 1b is a local minimum of the ground-state energy surface and is 0.25 eV (6.6 kcal/mol) higher in energy that the neutral structure of Figure 1a at the MP2/cc-pVDZ level. This energy difference is reduced to 0.21 eV (4.9 kcal/mol) when CC2/aug(N)-cc-pVDZ calculations are performed at the same geometries.

The two fairly short and strong hydrogen bonds ($\sim$1.7 Å) between water and the carboxylate and ammonium groups stabilize the zwitterionic form (Figure 1b). The hydrogen bridges in the neutral form exhibit a significant asymmetry (Figure 1a). Whereas the hydrogen bonds on the hydroxyl side are of similar length as in the zwitterionic form (1.66 and 1.82 Å), the hydrogen bonds on the carbonyl side are much weaker (1.96 and 2.07 Å). The strong hydrogen bonds on the hydroxyl side of Tyr$-W_2$ facilitate the transfer of the hydroxyl proton to the amino group via the water bridge, as will be discussed below.

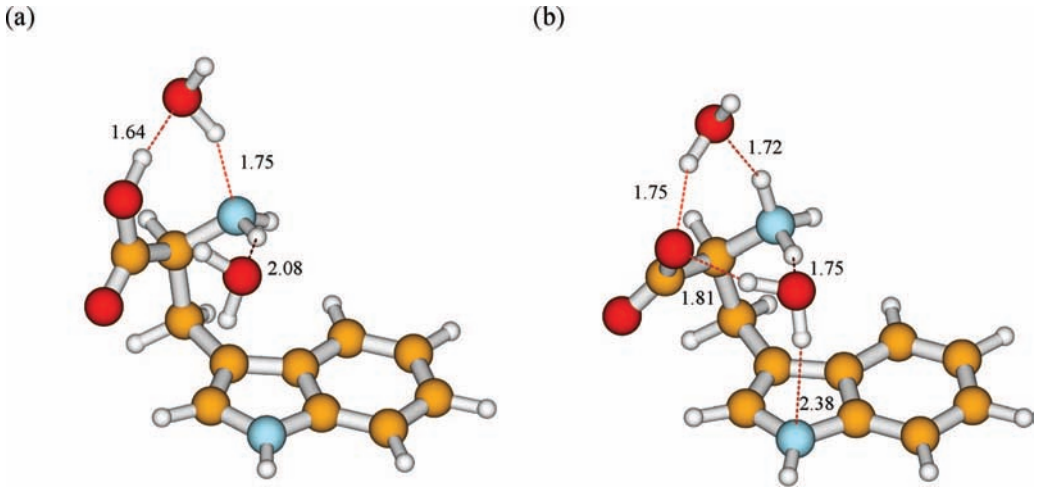

Figure 2. Ground-state equilibrium geometries of the neutral (a) and zwitterionic (b) forms of tryptophan−$(H_2O)_2$. Bond lengths are given in angstroms.

(ii) Trp−W₂. The equilibrium structures of the neutral and zwitterionic forms of Trp−W_2, obtained by unconstrained geometry optimization of the ground-state energy at the MP2/cc-pVDZ level, are shown in panels a and b, respectively, of Figure 2. The Cartesian geometry parameters of these structures are given in the Supporting Information. The zwitterionic structure shown in Figure 2b is a local minimum of the ground-state energy surface and is 0.08 eV (2.1 kcal/mol) lower in energy than the neutral structure in Figure 2a at the MP2/def-SV(P) level. The energy order is reversed when CC2/aug(N)-cc-pVDZ calculations are performed on the same geometry. The zwitterionic form is by 0.11 eV (2.9 kcal/mol) less stable than the neutral form.

The zwitterionic form involves four short and strong hydrogen bonds between the water and the carboxylate and ammonium groups (1.7−1.8 Å) (see Figure 2b). Trp−W_2 has an additional weak hydrogen bond compared to tyrosine: One of the water molecules is hydrogen-bonded to the nitrogen of the indole ring. The distance is 2.38 Å. In the neutral form, one water molecule exhibits strong hydrogen bonds. The hydrogen bond between the hydroxyl group and water (1.64 Å) is shorter than the hydrogen bond between the water and the amino group (1.75 Å). The strongly bonded water molecule is actively involved in the water bridge and can mediate the transfer of a proton from the carboxyl group to the amino group. The other water molecule is involved in a single weak hydrogen bond (distance = 2.08 Å). This water molecule slightly changes orientation upon proton transfer. It has a stabilizing effect on the zwitterionic structure in the excited state. The latter is unstable when fewer than two water molecules are attached.

3.2. Relative Energies, Excitation Energies, Molecular Orbitals. ***(i) Tyr−W₂.*** The vertical excitation energies, oscillator strengths, and dipole moments of the neutral and zwitterionic forms of Tyr−W_2 are given in Table 1. As expected, the ground state of the zwitterionic form is considerably more polar than the ground state of the neutral form. The absorption spectra of both forms are dominated by local $\pi \rightarrow \pi^*$ transitions within the aromatic ring (L_b and L_a states). The lowest excited singlet state of both forms, $S_1(L_b)$, is vertically well separated from the optically dark S_2 state, which results from the transition between molecular orbitals localized on the amino acidic moiety of the system.

The molecular orbitals involved in the electronic excitation to the lowest singlet states of the neutral and zwitterionic forms of Tyr−W_2 are shown in Figures 3 and 4, respectively. Although the π orbital involved in the $L_b(\pi\pi^*)$ excitation of both forms is essentially localized on the phenyl ring (Figures 3a and 4a), the π^* orbital contains a substantial admixture of Rydberg orbitals localized on the NH_2 or NH_3^+ moieties (Figures 3c and 4c, respectively). The S_2 state of the neutral form of Tyr−W_2

TABLE 1: Vertical Excitation Energies (Δ*E*), Oscillator Strengths (*f*), and Dipole Moments (*μ*) of the Neutral and Zwitterionic Forms of the Tyr−W_2 System, Calculated with the CC2/aug(N)-cc-pVDZ Method at the MP2/cc-pVDZ Geometry

state	Δ*E* (eV)	*f*	*μ* (D)
	Neutral Form		
S_0			3.89
$^1L_b(\pi\pi^*)$	4.93 (4.68)[b]	0.03	4.37 (4.37)[d]
$n_{COO}\sigma_{Am}^*$	5.85 (4.22)[b]	0.003	3.41 (3.67)[d]
$^1L_a(\pi\pi^*)$	6.21	0.21	5.49
	Zwitterionic Form		
S_0	(0.21)[a]		7.1
$^1L_b(\pi\pi^*)$	5.0 (4.87)[b]	0.03	7.4 (7.24)[d]
$n_{COO}{}^+\sigma_{Am}^*$	5.6 (4.03)[c]	0.00	3.2 (6.11)[d]
$\pi_{COO}{}^-\sigma_{Am}^*$	5.7	0.00	4.3
$^1L_a(\pi\pi^*)$	6.2	0.11	5.3

[a] Relative to the ground-state minimum of the neutral form. [b] Adiabatic energy. [c] Adiabatic energy calculated at R_{CN} = 1.5 Å. [d] Calculated at the minimum energy of a given state.

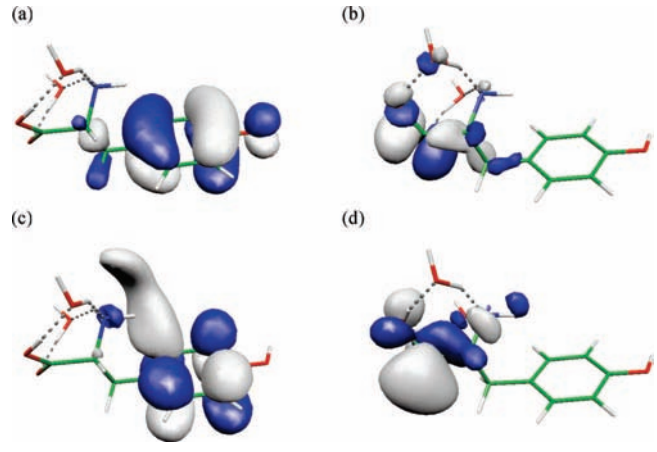

Figure 3. Singly occupied molecular orbitals in the $^1L_b(\pi\pi^*)$ state (a, c) and in the $^1n\pi^*$ state (b, d) of the neutral form of tyrosine−$(H_2O)_2$ determined at the equilibrium geometry of the respective state.

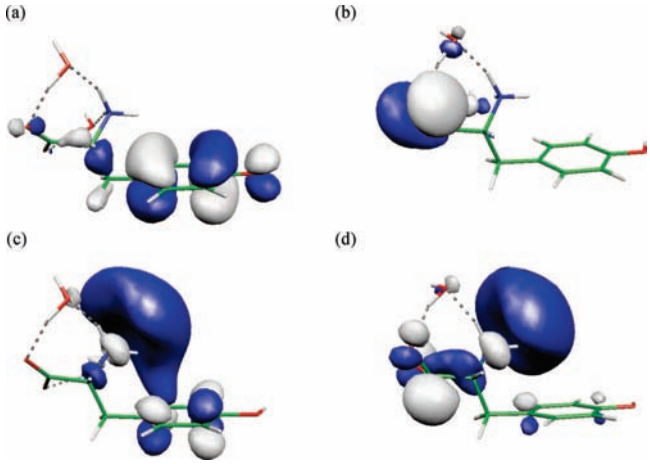

Figure 4. Singly occupied molecular orbitals in the $^1L_b(\pi\pi^*)$ state (a, c) and in the $^1n\pi^*$ state (b, d) of the zwitterionic form of tyrosine$-(H_2O)_2$ determined at the minimum-energy geometry of the respective state.

TABLE 2: Vertical Excitation Energies (ΔE), Oscillator Strengths (f), and Dipole Moments (μ) of the Neutral and Zwitterionic Forms of the Trp$-W_2$ System Calculated with the CC2/aug(N)-cc-pVDZ Method at the MP2/cc-pVDZ Geometry

state	ΔE (eV)	f	μ (D)
	Neutral Form		
S_0			2.22
$^1L_b(\pi\pi^*)$	4.87	0.03	1.26
$^1L_a(\pi\pi^*)$	4.96 (4.48)[b]	0.08	2.56 (3.66)[d]
$n_{COO}\pi^*_{COO}/n_{COO}\sigma_{Am}^*$	5.82	0.0005	4.87
	Zwitterionic Form		
S_0	(0.08)[a]		5.02
$^1L_b(\pi\pi^*)$	4.88 (4.64)[b]	0.02	4.40 (4.63)[d]
$^1L_a(\pi\pi^*)$	4.96	0.07	1.09
$\pi_{COO}\sigma_{Am}^*$	5.59	0.007	5.25
$n_{COO}\sigma_{Am}^*$	5.84 (3.93)[c]	0.001	7.85 (5.32)[d]

[a] Relative to the ground-state minimum of the neutral form. [b] Adiabatic energy. [c] Adiabatic energy calculated at $R_{CN} = 1.5$ Å. [d] Calculated at the minimum energy of a given state.

involves a local excitation from the lone pair orbital n_{COO} (Figure 3b) to the π^* orbital (Figure 3c) mostly localized on the same moiety. This is not the case for the S_2 state of the zwitterionic form, which involves a significant charge transfer from the lone pair of the COO^- group (Figure 4b) to the orbital, which is a mixture of a π^* orbital localized on the CH_2COO^- moiety and a diffuse σ^* orbital largely localized on the NH_3^+ group (Figure 4d). These states are of importance for the photophysical behavior to be discussed below. During the transition from the neutral form to the zwitterionic form (see also the discussion below) the character of this state switches from initially being mostly an $n\pi^*$ state to an $n\sigma^*_{Am}$ state. In the following discussion, this state is labeled $n\pi^*$ or $n\sigma^*_{Am}$, depending on the main character of this state at the considered geometry.

Both forms of Tyr$-W_2$ represent also local minima on the PE surface of the lowest excited singlet state (L_b) at the CC2/def-SV(P) level of theory. As in the ground state, the zwitterionic form is less stable than the neutral one in the S_1 state by 0.19 eV (4.3 kcal/mol) (see Table 1). The energy of this state is stabilized only slightly upon geometry optimization. This is not the case for the S_2 state. The adiabatic energy of this state is about 1.6 eV lower than its vertical energy (Table 1), and this state is adiabatically the lowest excited singlet state of the system. Examination of the geometry of this state (see Supporting Information) shows that the stabilization energy results from the elongation of the C═O bond (by about 0.25 Å). The barrier, which separates both forms of Tyr$-W_2$ in this state, is vanishingly small. It is found that the zwitterionic form is unstable in this state and relaxes by the detachment of ammonia (see below).

(ii) Trp$-W_2$. The vertical excitation energies, oscillator strengths, and dipole moments of the neutral and zwitterionic form of Trp$-W_2$ are given in Table 2. As in Tyr$-W_2$, the zwitterionic structure is more polar than the neutral structure. The two lowest excited states of both forms are the ^1L_b and ^1L_a states associated with the indole chromophore. The energetic difference of these states is <0.1 eV. The ^1L_a state is considerably lower in energy than in Tyr$-W_2$, where it is about 1.2 eV above the ^1L_b state. The oscillator strengths of the ^1L_a and ^1L_b states in Trp$-W_2$ are similar, differing only by a factor of 3. This indicates that the ^1L_a and ^1L_b states of the indole chromophore are mixed by the amino acid group. Nevertheless, we assign the first excited state as ^1L_b and the second state as ^1L_a. This assignment is based on the comparison of the oscillator strengths, the dipole moments, and the characters of the MOs. Note that the ^1L_a state has a low dipole moment in the zwitterionic form. The low dipole moment results from the cancellation of a high dipole moment of the indole ring and an almost antiparallel dipole moment of the alanyl side chain. The third excited state is well separated from the two $\pi\pi^*$ states in both forms of Trp$-W_2$. The former is at almost the same energy as in Tyr$-W_2$ and results from a transition in the amino acidic moiety. The energy of this state is not affected by the identity of aromatic residue and should therefore exist in all amino acids.

The molecular orbitals involved in these excitations can be found in the Supporting Information (see Figure 1 for orbitals of the neutral form and Figure 2 for orbitals of the zwitterionic form). The orbitals that are involved in the ^1L_b and ^1L_a states are π orbitals located on the indole ring. The third excited state of the neutral form involves an excitation from the lone pair orbital n_{COO} to the π^* orbital one the same group, similar to Tyr$-W_2$. In the zwitterionic form, the third excited state involves a charge transfer from the π orbital localized on the COO^- group to a diffuse σ^* orbital on the NH_3^+ group. The fourth state involves an excitation from the lone pair of the COO^- group to a diffuse σ^* orbital on the NH_3^+ group. These states also exist in similar form in the Tyr$-W_2$ system, but their order is inverted in Trp$-W_2$ and their energies are closer to each other.

The optimization of the geometry of the excited state in the neutral form and the zwitterionic form leads to different states. The S_1 minimum in the neutral form is of ^1L_a character, whereas it is of ^1L_b character for the zwitterionic form. This state inversion is a result of the mixing of both states as discussed above. It is known that the polar ^1L_a state is stabilized more than the ^1L_b state in bulk water. Therefore, it is expected that additional water molecules will stabilize the ^1L_a state in the zwitterionic form and will bring this state below the ^1L_b state.

3.3. Proton-Transfer Reaction Path. ***(i) Tyr$-W_2$.*** In Figure 5, the energy profiles of two reaction paths are shown. The first connects the neutral and zwitterionic forms of Tyr$-W_2$ (Figure 5a). The second leads to the detachment of ammonia in the zwitterionic form (Figure 5b). We have determined these reaction paths on the S_0 surface as well as on the S_1 and S_2 surfaces. The energy profiles computed along these coordinate-driven minimum-energy paths (MEPs) are designated S_0, ^1L_b, and $^1n\pi^*$, respectively. The energy profile of the S_0 state, computed along the MEPs in the $^1\pi\pi^*$ and $^1n\pi^*$ states, is also

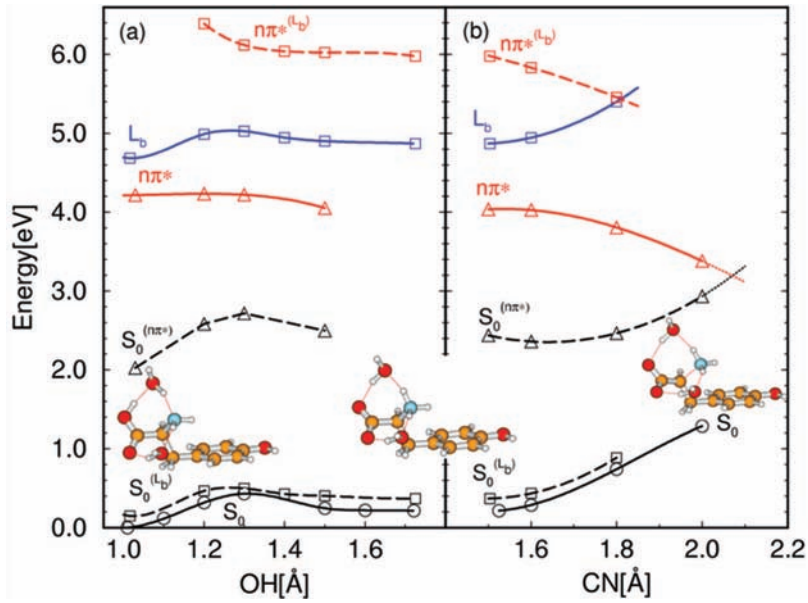

Figure 5. Minimum-potential-energy profiles of the S_0 state (circles), the $L_b(\pi\pi^*)$ singlet state (squares), and the $^1n\pi^*$ state (triangles) of tyrosine$-(H_2O)_2$ as a function of the hydrogen transfer (a) and of the NH_3 detachment (b) reaction coordinates: (solid lines) energy profiles of reaction paths determined in the same electronic state; (dashed line) energy of the ground state calculated at the geometry of the $L_b(\pi\pi^*)$ state (squares) and $^1n\pi^*$ state (triangles) (designated $S_0^{(\pi\pi^*)}$ and $S_0^{(n\pi^*)}$); (dot-dashed line with squares) energy of the $^1n\pi^*$ state calculated at the geometry of the $L_b(\pi\pi^*)$ state ($^1n\pi^{*(\pi\pi^*)}$). Colors: S_0, black; ^1L_b, blue; $^1n\pi^*$, red.

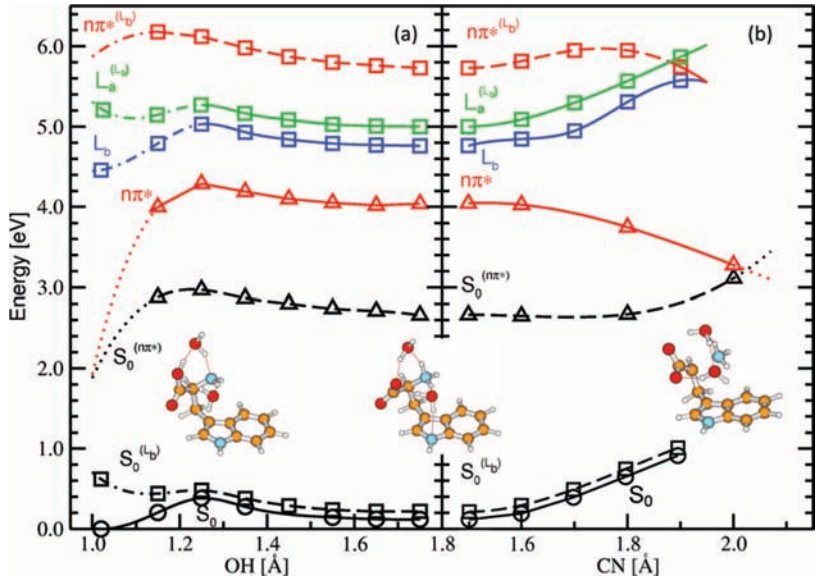

Figure 6. Minimum-potential-energy profiles of the S_0 state (circles) and of the $L_b(\pi\pi^*)$ singlet state and L_a ($\pi\pi^*$) singlet state (squares) and of the $^1n\pi^*$ state (triangles) of tryptophan$-(H_2O)_2$ as a function of the hydrogen transfer (a) and of the NH_3 detachment (b) reaction coordinates: (solid lines) energy profiles of reaction paths determined in the same electronic state; (dashed line) energy of the ground state calculated at the geometry of the $L_b(\pi\pi^*)$ state (squares) and $^1n\pi^*$ state (triangles) (designated $S_0^{(\pi\pi^*)}$ and $S_0^{(n\pi^*)}$); (dot-dashed line with squares) energy of the $^1n\pi^*$ state calculated at the geometry of the $L_b(\pi\pi^*)$ state ($^1n\pi^{*(\pi\pi^*)}$). Colors: S_0, black; ^1L_b, blue; ^1L_a, green; $^1n\pi^*$, red.

shown by the dashed lines designated $S_0^{(\pi\pi^*)}$ and $S_0^{(n\pi^*)}$, respectively. In addition, the energy profile of the $^1n\pi^*$ state, computed along the MEP determined in the $^1\pi\pi^*$ state (denoted $^1n\pi^{*(\pi\pi^*)}$), is given. For simplicity, the state $n_{COO}{}^+\sigma_{Am}{}^*$ is designated $n\pi^*$ throughout.

The reaction path that connects the neutral and zwitterionic forms of Tyr$-W_2$ corresponds to the transfer of a proton from the hydroxyl group through the water bridge to the amino group. It is represented in Figure 5a by the variation of the OH distance of the hydroxyl group. Inspection of this figure shows that the zwitterionic structure is higher in energy than the neutral structure in the electronic ground state, as discussed above. The barrier for conversion from the zwitterionic structure to the neutral structure is about 0.2 eV (4.5 kcal/mol) at this computational level (CC2/aug(R_N)-cc-pVDZ). The minimum-energy profile of the $L_b(\pi\pi^*)$ is largely parallel to that of the ground state. This is not the case for the $^1n\pi^*$ state. In this state, the neutral form of Tyr$-W_2$ is separated by a vanishingly small barrier from the zwitterionic form. The barrier is below the zero-point vibrational energy. Moreover, for larger values of the OH distance (OH > 1.5 Å), a spontaneous detachment of ammonia takes place.

(ii) Trp$-W_2$. The energy profiles of the reaction path connecting the neutral and zwitterionic structures of Trp$-W_2$ are shown in Figure 6a. The zwitterionic structure is higher in energy than the neutral form in the ground state, as discussed

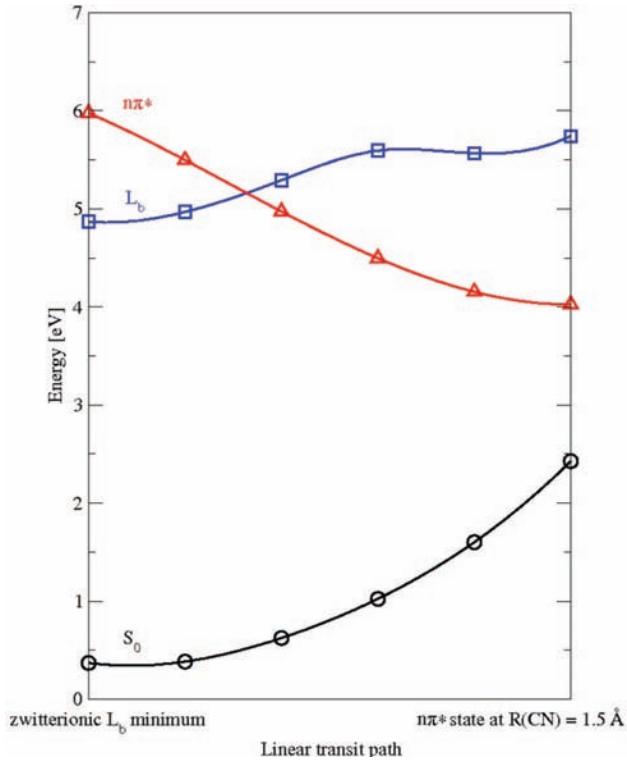

Figure 7. Linear transit path between the L_b minimum of the zwitterionic Tyr−W_2 and the nπ* state at the fixed C−N distance of 1.5 Å. The L_b state is denoted by squares, the nπ* state is denoted by triangles, and the S_0 state is denoted by circles. Colors: S_0, black; L_b, blue; nπ*, red.

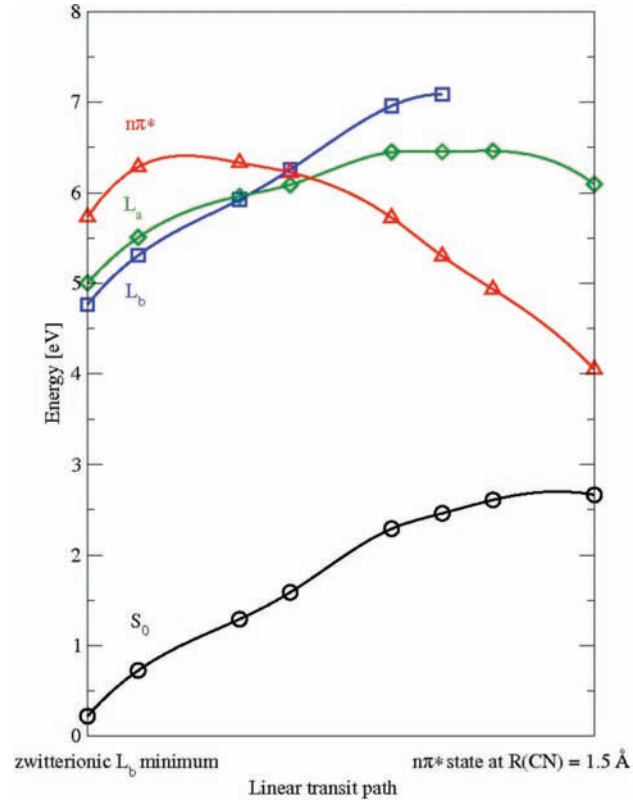

Figure 8. Linear transit path between the L_b minimum of the zwitterionic Trp−W_2 and the nπ* state at the fixed C−N distance of 1.5 Å. The L_b state is denoted by squares, the L_a state is denoted by diamonds, the nπ* state is denoted by triangles, and the S_0 state is denoted by circles. Colors: S_0, black; L_b, blue; L_a, green; nπ*, red.

above. The barrier for conversion from the neutral form to the zwitterionic form is about 0.25 eV (5.5 kcal/mol), slightly higher than in Tyr−W_2. The energy profiles of both $\pi\pi$* states are nearly parallel to the energy profile of the S_0 state. The optimized first excited state of the neutral form is the ^1L_a state. Near the Franck−Condon region, the first and second singlet states are mixed and can therefore not uniquely be assigned as ^1L_b and ^1L_a. They are therefore drawn as dashed lines. The S_0 energy is also represented by a dashed line in this region, because it cannot clearly be assigned whether the related optimized state is the ^1L_b or the ^1L_a state. Another difference with respect to Tyr−W_2 is the optimized nπ* state (denoted by red triangles) in the Franck−Condon region. At short OH distances, the geometry of the ^{1}nπ* state could not be optimized. The optimization of the ^{1}nπ* energy leads to a conical intersection with the ground state, where the carbonyl oxygen attaches to the carbon atom adjacent to the nitrogen atom of the indole ring, forming a six-membered ring (see Figure 3 in the Supporting Information). The nπ* energy is therefore drawn as dotted line in this region. Extrapolation of this line and the S_0 line leads to the described ^{1}nπ*-S_0 conical intersection.

3.4. C−N Stretching Reaction Path. ***(i) Tyr−W₂.*** The mechanistic explanation of the dissociation of the C_α−N bond is as follows: the $n_{COO}\sigma_{Am}$* electronic excitation of the zwitterionic structure transfers electronic charge from the COO^- group toward the NH_3^+ moiety. The partial neutralization of NH_3^+ weakens the C−N bond, resulting in the detachment of neutral NH_3. We therefore consider the minimum-energy reaction path for C−N stretching, starting from the zwitterionic structure. The PE profiles calculated along this reaction path in the two lowest excited singlet states are shown in Figure 5b. In analogy to Figure 5a, the PE profiles of the ground state calculated along the minimum-energy paths determined in the $^1\pi\pi$* and ^{1}nσ* states are also shown (dashed lines). Let us mention that the nominal ^{1}nσ* state of the zwitterionic form is designated ^{1}nπ* in Figure 5b for consistency with the notation used in Figure 5a. As will be discussed below, this state restores the ^{1}nπ* character along the C−N stretching coordinate.

As expected, the lengthening of the C−N bond is energetically unfavorable in the electronic ground state and in the $^1L_b(\pi\pi^*)$ state. In the ^{1}nσ*/^{1}nπ* state, on the other hand, we find a barrierless energy profile for the dissociation of the C−N bond. It can be seen that the extrapolation of the ^{1}nσ*/^{1}nπ* and $S_0^{(n\sigma^*)}$ profiles beyond the last converged CC2 calculation (at R_{CN} = 2.0 Å) results in their intersection. This intersection is a true intersection (conical intersection), because these energies are calculated at the same geometries.

(ii) Trp−W₂. The energy profile of the same reaction path in Trp−W_2 is shown in Figure 6b. The results obtained for Trp−W_2 are rather similar to the Tyr−W_2 system. The main difference is that the energy of the ^{1}nπ* state calculated at the ^1L_b optimized geometry exhibits a barrier of about 0.2 eV.

The CC2 method, being a single-reference method, is expected to fail in the vicinity of the intersection of excited states with the electronic ground state. The corresponding regions of the PE profiles are given by dotted lines in Figures 5b and 6b, indicating that these data are less reliable. The accurate calculation of the PE surfaces in the immediate vicinity of S_1−S_0 conical intersections requires multireference methods, in particular, state-averaged CASSCF and multireference perturbation or configuration−interaction methods. The existence of a ^{1}nπ*−S_0 conical intersection near R_{CN} = 2.1 Å was confirmed for the Gly−W_2 system by the direct optimization of the intersection geometry at the CASSCF level.[53] Because

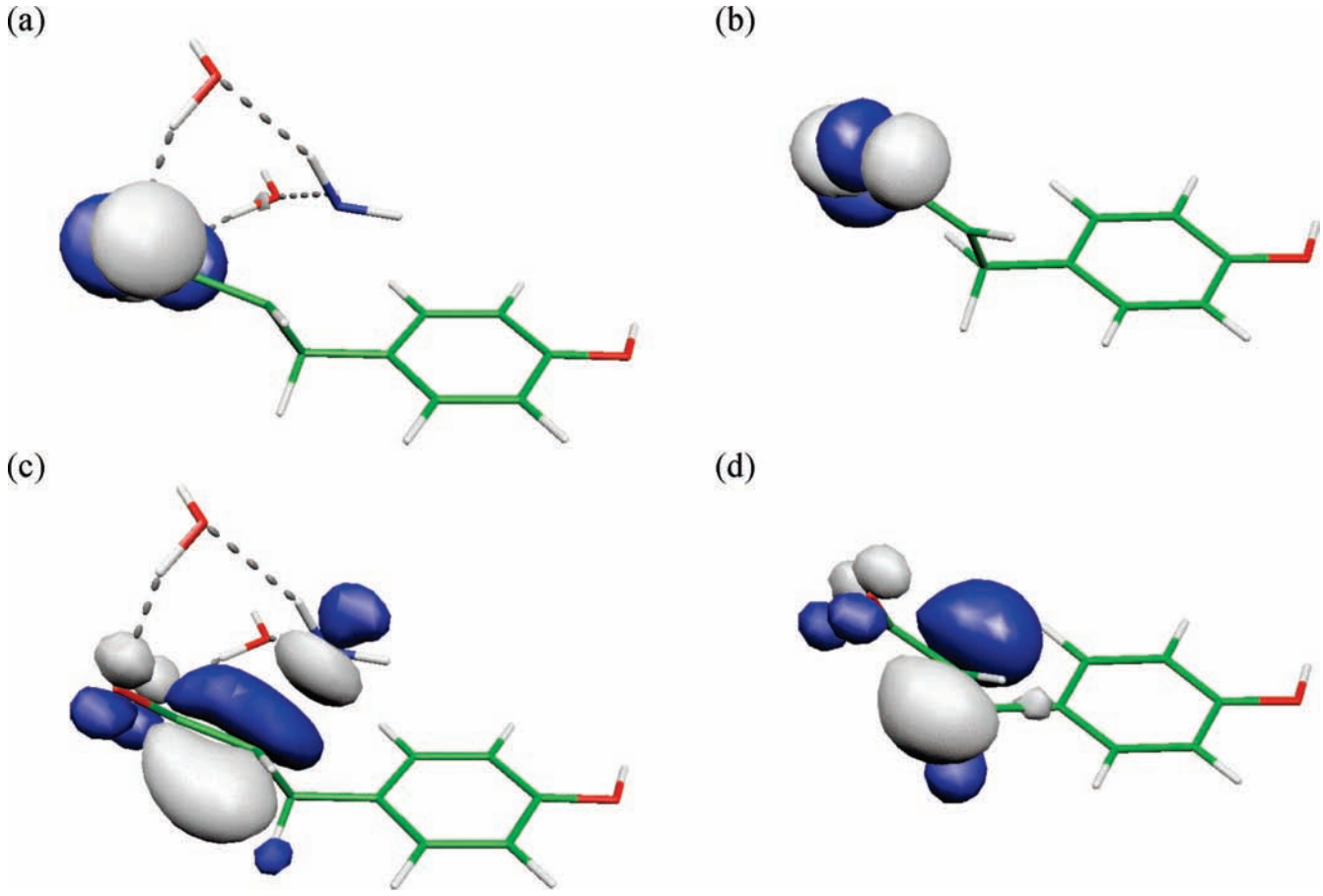

Figure 9. Singly occupied molecular orbitals of the $^1n\pi^*$ state of the zwitterionic form of tyrosine$-(H_2O)_2$ determined at $R_{CN} = 2.0$ Å on the minimum-energy reaction path in this state (a, c). The singly occupied molecular orbitals of the lowest triplet state of the $O_2C-CH_2-C_6H_4OH$ biradical are shown in (b) and (d).

the geometric changes that lead to the intersection are confined to the amino acidic moiety, the same conical intersection is expected to exist in Tyr$-W_2$ and Trp$-W_2$ systems. It is expected to represent a generic feature of amino acids in an aqueous environment.

3.5. Estimation of the Deamination Barrier. ***(i) Tyr$-W_2$.*** The vertical excitation of the zwitterionic structure leads to the L_b state. The optimized $n\pi^*$ state lies below the L_b state, but has a much lower oscillator strength than the L_b state. Additionally, the equilibrium geometries of these states differ from each other. It is expected that the excitation of the L_b state is followed by an internal conversion to the $n\pi^*$ state. We have estimated the barrier for the internal conversion from the L_b state to the $n\pi^*$ state by calculating the energy profiles along the linear transit path between both equilibrium geometries. In particular, we calculated the linear transit path from the minimum of the L_b state to the minimum of the $n\pi^*$ state with the constraint of a fixed C$-$N distance of 1.5 Å. It is not possible to construct the linear transit path ending at the freely optimized $n\pi^*$ state, because this state is dissociative, as can be seen from Figures 5 and 6. The energy profile of the linear transit path for the Tyr$-W_2$ cluster is shown in Figure 7. The vertical excitation by a photon leads to the L_b state. Along the linear transit path, the energy of the $n\pi^*$ state is lowered considerably, whereas the energy of the L_b state is rather flat. The L_b-$n\pi^*$ crossing is about 0.3 eV above the L_b minimum. The energy of L_b-$n\pi^*$ is an upper limit of the actual barrier, because the linear transit path is not the minimum-energy path. For this system, the L_a state is not relevant, because it lies above the $n\pi^*$ state (see previous sections for more details).

(ii) Trp$-W_2$. The linear transit path for the Trp$-W_2$ cluster has been constructed in the same way as for the Tyr$-W_2$ cluster. The energy profiles along the linear transit path are shown in Figure 8. In this system, the L_a and L_b states are almost isoenergetic at the zwitterion equilibrium geometry. Along the linear transit path, the energies of the L_a and L_b states rise. The energies of the L_b and L_a states interchange along the linear transit path. Near the crossing with the energy of the $n\pi^*$ state, all three states are almost degenerate. This finding indicates the existence of a three-fold conical intersection. The barrier for L_b-$n\pi^*$ interconversion is estimated to be about 1.4 eV. The construction of this linear transit path was difficult, because the water molecules are arranged differently in the initial and final structures. It is expected that the geometries along the minimum-energy path can be rather different from those in the linear transit path. Therefore, the actual barrier may be smaller than estimated by this linear transit path. Nevertheless, the barrier in Trp$-W_2$ is most likely higher than the barrier in Tyr$-W_2$. It is therefore anticipated that the yield of ammonia is higher in Tyr$-W_2$ than in Trp$-W_2$.

3.6. Frontier Orbitals of Tyr$-W_2$. To provide insight into the electronic mechanisms leading to the detachment of ammonia from zwitterionic Tyr$-W_2$, we display in Figure 9 the frontier molecular orbitals at relevant nuclear structures. At the ground-state equilibrium geometry of the zwitterionic form, the lowest excited singlet state is dominated by the electronic excitation from the lone pair orbital of the carboxyl group (Figure 4b) to the lowest unoccupied (in the Hartree$-$Fock reference) molecular orbital (Figure 4d). The latter orbital can be recognized as a combination of the π^* orbital of the carboxyl

group with a diffuse σ^* orbital on the NH_3 group. The σ^* orbital is seen to be antibonding with respect to the free (not hydrogen-bonded) NH bond of ammonia. Excitation to this nominally nσ^* state may result in the detachment of a hydrogen atom from the NH_3 group by a mechanism which is similar to that occurring in aromatic chromophores (the so-called $\pi\sigma^*$ mechanism[54]). However, the stretching of the N−H distance leads to the localization of this orbital on the O_2C-CH_2 fragment in the form of a valence π^*-type orbital (Figure 9c), whereas the form of the lone pair orbital n (Figure 9a) is little affected by the stretching of the C−N bond. These orbitals of the Tyr−W_2 system are essentially identical with the orbitals obtained for the planar $O_2C-CH_2-C_5H_4OH$ moiety alone (Figure 9b,d).

The $O_2C-CH_2-C_5H_4OH$ molecule has an interesting electronic structure. Its ground state is a triplet state of biradicalic character with two unpaired electrons residing in the n (Figure 9b) and π^* (Figure 9d) orbitals, respectively (^{3}nπ^* state). The lowest closed-shell state (with two electrons in the lone pair orbital) lies >2 eV above the ground state (CC2 result). The intersection of the S_1 and S_0 energies along the coordinate for detachment of ammonia (Figure 3b) thus results from an intrinsic property of the $O_2C-CH_2-C_5H_4OH$ fragment, which is temporarily formed in the course of the photochemical reaction.

4. Conclusions

The photophysical and photochemical reaction mechanisms in the lowest excited singlet states of the Tyr−W_2 and Trp−W_2 clusters have been investigated with computational methods. As expected, the transfer of the proton from the neutral covalent structure of Tyr−W_2 and Trp−W_2 to the zwitterionic structure is found to be endothermic in the electronic ground state and to involve, moreover, a barrier of about 5 kcal/mol. A similar energy profile is predicted for proton transfer in the lowest $^1\pi\pi^*$ state of Tyr−W_2 and Trp−W_2.

In the lowest singlet state of nπ^* character, on the other hand, the proton-transfer reaction from the neutral to the zwitterionic structure is predicted to be slightly exothermic in both Tyr−W_2 and Trp−W_2. The energy profile of this reaction path is barrierless in Tyr−W_2, whereas a barrier of about 4.6 kcal/mol exists in Trp−W_2. In both cases, the ^{1}nπ^* state associated with the peptide chain becomes the S_1 state upon geometry optimization. The proton transfer in Tyr−W_2 and Trp−W_2 does not lead to crossings of the singlet potential-energy surfaces, neither among the excited states nor between the excited states and the ground state (see Figures 5a and 6a).

The most interesting finding of the present work is the prediction of a reaction path corresponding to the detachment of neutral NH_3 for the zwitterionic structures of Tyr−W_2 and Trp−W_2. In both systems, this path leads to a low-lying conical intersection of the S_1 and S_0 potential-energy surfaces. This conical intersection can either effect rapid radiationless decay back to the electronic ground state, or, if the conical intersection is passed diabatically, lead to detachment of neutral NH_3. This mechanism can explain the enhanced fluorescence quenching in Tyr and Trp in aqueous solution at neutral and acidic pH[4,6,22−24] as well as the relatively high quantum yields for deamination.[1−6]

The UV-absorbing states in both Tyr and Trp are the $^1\pi\pi^*$ states of the aromatic chromophores. Whereas the first $^1\pi\pi^*$ state is the lowest excited singlet state in vertical electronic excitation of Tyr and Trp, the lowest ^{1}nπ^* state becomes the S_1 state upon geometry optimization (see Figures 5a and 6a). This implies that there exists a seam of intersection of the potential-energy surfaces of the $^1\pi\pi^*$ state and the ^{1}nπ^* state. The initially populated $^1\pi\pi^*$ state of the chromophore thus can internally convert to the ^{1}nπ^* state of the peptide chain. The present results (see Figures 6 and 7) indicate that the $^1\pi\pi^*$ state to the ^{1}nπ^* internal conversion occurs more easily in Tyr−W_2 than in Trp−W_2. On the S_1(nπ^*) energy surface, a barrierless or nearly barrierless proton-transfer reaction path leads to the zwitterionic structures (see Figures 5a and 6a) and from there to the S_1-S_0 conical intersection via C_α−N stretching (see Figures 5b and 6b). This reaction mechanism for internal conversion and/or deamination is in competition with hydrogen detachment from phenol/indole via $^1\pi\sigma^*$ states.[47,55] The spectroscopic investigation of these competing photochemical processes in Tyr−water and Trp−water clusters can provide insight into the poorly understood photochemistry of Tyr and Trp in aqueous solution.

An alternative mechanism of fluorescence quenching in (bare) zwitterionic Trp has been investigated by Blancafort et al. with CASSCF and CAS-MP2 methods.[56] This mechanism involves hydrogen transfer from (the partially neutralized) NH_3^+ group to a carbon atom in the indole ring, as has been suggested by Robbins et al.[22] (see also refs 57−59). It has been predicted that this reaction path also leads to an S_1-S_0 conical intersection and may contribute to fluorescence quenching. This reaction mechanism may possibly compete with the NH_3-loss channel (the minimum-energy path and its energy profile have not been determined in ref 56).

The present results for the zwitterions of Tyr and Trp may be compared with recent spectroscopic and computational results for protonated Tyr and Trp in the gas phase.[47,55,60−64] Kang et al. have shown by femtosecond pump−probe measurements that the $^1\pi\pi^*$ excited state of $TrpH^+$ possesses an extremely short lifetime.[61] Both hydrogen detachment and cleavage of the C_α−N bond have been identified.[61] Calculations have revealed the role of a low-lying $^1\pi\sigma^*$ state of pronounced charge-transfer character.[47,55,64] The partial neutralization of the NH_3^+ group results in the formation of a hypervalent radical, $C_\alpha-NH_3$, which has low barriers for dissociation by either H-bond rupture or C_α−N cleavage.[47,55] Both reaction coordinates lead to S_1-S_0 conical intersections. Slightly different barriers in $TyrH^+$ and $TrpH^+$ result in spectacular differences of the $^1\pi\pi^*$ spectra of cold $TyrH^+$ and $TrpH^+$.[63,64]

Acknowledgment. This work has been supported by the Deutsche Forschungsgemeinschaft (DFG) and the Ministry of Science and Education of Poland. D.S. is supported by a fellowship of the Alexander von Humboldt foundation. A.L.S. acknowledges partial support by a visitor grant of the DFG cluster of excellence "Munich Centre of Advanced Photonics" (www.munich-photonics.de).

Supporting Information Available: Cartesian geometry parameters and molecular orbitals of Tyr−W_2 and Trp−W_2, This information is available free of charge via the Internet at http://pubs.acs.org.

References and Notes

(1) Templer, H.; Thistlethwaite, P. J. *Photochem. Photobiol.* **1976**, *23*, 79.
(2) Holt, L. A.; Milligan, B.; Rivett, D. E.; Stewart, F. H. C. *Biochim. Biophys. Acta* **1977**, *499*, 131.
(3) Dillon, J. *Photochem. Photobiol.* **1980**, *32*, 37. *ibido* **1980**, *33*, 137.
(4) Creed, D. *Photochem. Photobiol.* **1984**, *39*, 537.
(5) Beecham, J. M.; Brand, L. *Annu. Rev. Biochem.* **1985**, *54*, 43.
(6) Creed, D. *Photochem. Photobiol.* **1984**, *39*, 563.
(7) Bent, T. V.; Hayon, E. *J. Am. Chem. Soc.* **1975**, *97*, 2599.
(8) Bent, T. V.; Hayon, E. *J. Am. Chem. Soc.* **1975**, *97*, 2612.
(9) Baugher, J. F.; Grossweiner, L. I. *J. Phys. Chem.* **1977**, *81*, 1349.

(10) Amouyal, E.; Bernas, A.; Grand, D. *Photochem. Photobiol.* **1979**, *29*, 1071.
(11) Grossweiner, L. I.; Brendzel, A. M.; Blum, A. *Chem. Phys.* **1981**, *57*, 147.
(12) Stevensen, K. L.; Papadantonakis, G. A.; Le Breton, P. R. *J. Photochem. Photobiol. A* **2000**, *133*, 159.
(13) Sherin, P. S.; Snytnikova, O. A.; Tsentalovich, Y. P. *Chem. Phys. Lett.* **2004**, *391*, 44.
(14) Katoh, R. *J. Photochem. Photobiol. A* **2007**, *189*, 211.
(15) Pino, G.; Gregoire, G.; Dedonder-Lardeux, C.; Jouvet, C.; Martrenchard, S.; Solgadi, D. *Phys. Chem. Chem. Phys.* **2000**, *2*, 893.
(16) Dedonder-Lardeux, C.; Grosswasser, D.; Jouvet, C.; Martrenchard, S. *PhysChemComm* **2001**, *4*, 1.
(17) Ishiuchi, S.; Daigoku, K.; Saeki, M.; Sakai, M.; Hashimoto, K.; Fujii, M. *J. Chem. Phys.* **2002**, *117*, 7077.
(18) Lippert, H.; Stert, V.; Hesse, L.; Schulz, C. P.; Hertel, I. V.; Radloff, W. *J. Phys. Chem. A* **2003**, *107*, 8239.
(19) Sobolewski, A. L.; Domcke, W. *Chem. Phys. Lett.* **2000**, *329*, 130.
(20) Sobolewski, A. L.; Domcke, W. *J. Phys. Chem. A* **2001**, *105*, 9279.
(21) Sobolewski, A. L.; Domcke, W. *Phys. Chem. Chem. Phys.* **2007**, *9*, 3818.
(22) Robbins, R. J.; Fleming, G. R.; Beddard, G. S.; Robinson, G. W.; Thistlethwaite, P. J.; Woolfe, G. J. *J. Am. Chem. Soc.* **1980**, *102*, 6271.
(23) Eftink, M. R.; Jia, Y.; Hu, D.; Ghiron, C. A. *J. Phys. Chem.* **1995**, *99*, 5713.
(24) Guzow, K.; Szabelski, M.; Rzeska, A.; Karolczak, J.; Sulowska, H.; Wiczk, W. *Chem. Phys. Lett.* **2002**, *362*, 519.
(25) Tassin, J. D.; Borkman, R. F. *Photochem. Photobiol.* **1980**, *32*, 577.
(26) Lion, Y.; Kuwabara, M.; Riesz, P. *Photochem. Photobiol.* **1982**, *35*, 53.
(27) Seidel, C.; Orth, A.; Greulich, K.-O. *Photochem. Photobiol.* **1993**, *58*, 178.
(28) Rizzo, T. R.; Park, Y. D.; Peteanu, L. A.; Levy, D. H. *J. Chem. Phys.* **1986**, *84*, 2534.
(29) Rizzo, T. R.; Park, Y. D.; Levy, D. H. *J. Chem. Phys.* **1986**, *85*, 6945.
(30) Peteanu, L. A.; Levy, D. H. *J. Phys. Chem.* **1988**, *92*, 6554.
(31) Phillips, L. A.; Levy, D. H. *J. Phys. Chem.* **1986**, *90*, 4921.
(32) Martinez, S. J., III.; Altano, J. C.; Levy, D. H. *J. Mol. Spectrosc.* **1992**, *156*, 421.
(33) Lindinger, A.; Toennies, J. P.; Vilesov, A. F. *J. Chem. Phys.* **1999**, *110*, 1429.
(34) Piuzzi, F.; Dimicoli, L.; Mons, M.; Tardivel, B.; Zhao, Q. *Chem. Phys. Lett.* **2000**, *320*, 282.
(35) Snoek, L. C.; Kroemer, R. T.; Hockridge, M. R.; Simons, J. P. *Phys. Chem. Chem. Phys.* **2001**, *3*, 1819.
(36) Cohen, R.; Brauer, B.; Nir, E.; Grace, L.; de Vries, M. S. *J. Phys. Chem. A* **2000**, *104*, 6351.
(37) Aikens, C. M.; Gordon, M. S. *J. Am. Chem. Soc.* **2006**, *128*, 12835.
(38) Teh, C. K.; Sipior, J.; Sulkes, M. *J. Phys. Chem.* **1989**, *93*, 5393.
(39) Snoek, L. C.; Kroemer, R. T.; Simons, J. P. *Phys. Chem. Chem. Phys.* **2002**, *4*, 2130.
(40) Carcabal, P.; Kroemer, R. T.; Snoek, L. C.; Simons, J. P.; Bakker, J. M.; Compagnon, I.; Meijer, G.; von Helden, G. *Phys. Chem. Chem. Phys.* **2004**, *6*, 4546.
(41) Blom, M. N.; Compagnon, I.; Polfer, N. C.; von Helden, G.; Meijer, G.; Suhai, S.; Paizs, B.; Oomens, J. *J. Phys. Chem. A* **2007**, *111*, 7309.
(42) Christiansen, O.; Koch, H.; Jorgensen, P. *Chem. Phys. Lett.* **1995**, *243*, 409.
(43) Hättig, C.; Weigend, F. *J. Chem. Phys.* **2000**, *113*, 5154.
(44) Schreiber, M.; Silva-Junior, M. R.; Sauer, S. P. A.; Thiel, W. *J. Chem. Phys.* **2008**, *128*, 134110.
(45) Fleig, T.; Knecht, S.; Hättig, C. *J. Phys. Chem. A* **2007**, *111*, 5482–5491.
(46) Georgieva, I.; Trendafilova, N.; Aquino, A.; Lischka, H. *J. Phys. Chem. A* **2007**, *111*, 127–135.
(47) Gregoire, G.; Jouvet, C.; Dedonder, C.; Sobolewski, A. *J. Am. Chem. Soc.* **2007**, *129*, 6223–6231.
(48) Busker, M.; Nispel, M.; Häber, T.; Kleinermanns, K.; Etinski, M.; Fleig, T. *ChemPhysChem* **2008**, *9*, 1570–1577.
(49) Hättig, C. *J. Chem. Phys.* **2003**, *118*, 7751.
(50) Köhn, A.; Hättig, C. *J. Chem. Phys.* **2003**, *119*, 5021.
(51) Ahlrichs, R.; Bär, M.; Häser, M.; Horn, H.; Kölmel, C. *Chem. Phys. Lett.* **1989**, *162*, 165.
(52) Schaefer, A.; Horn, H.; Ahlrichs, R. *J. Chem. Phys.* **1992**, *97*, 2571.
(53) Sobolewski, A. L.; Domcke, W. *Chem. Phys. Lett.* **2008**, *457*, 404.
(54) Sobolewski, A. L.; Domcke, W.; Dedonder-Lardeux, C.; Jouvet, C. *Phys. Chem. Chem. Phys.* **2002**, *4*, 1093.
(55) Gregoire, G.; Jouvet, C.; Dedonder-Lardeux, C.; Sobolewski, A. L. *Chem. Phys.* **2006**, *324*, 398.
(56) Blancafort, L.; Gonzales, D.; Olivucci, M.; Robb, M. A. *J. Am. Chem. Soc.* **2002**, *124*, 6398.
(57) Saito, I.; Sugiyama, H.; Yamamoto, A.; Muramatsu, S.; Matsuura, T. *J. Am. Chem. Soc.* **1984**, *106*, 4286.
(58) Philips, L. A.; Webb, S. P.; Martinez, S. J., III.; Fleming, G. R.; Levy, D. H. *J. Am. Chem. Soc.* **1988**, *110*, 1352.
(59) Ruggiero, A. J.; Todd, D. C.; Fleming, G. R. *J. Am. Chem. Soc.* **1990**, *112*, 1003.
(60) Nolting, D.; Marian, C.; Weinkauf, R. *Phys. Chem. Chem. Phys.* **2004**, *6*, 2633.
(61) Kang, H.; Dedonder-Lardeux, C.; Jouvet, C.; Martrenchard, S.; Gregoire, G.; Desfrancois, C.; Schermann, J. P.; Barat, M.; Fayeton, J. A. *Phys. Chem. Chem. Phys.* **2004**, *6*, 2628; *ibid* **2005**, 7, 349; *ibid* **2005**, *7*, 2417.
(62) Talbot, F. O.; Tabarin, T.; Antoine, R.; Broyer, M.; Dugourd, P. *J. Chem. Phys.* **2005**, *122*, 074310.
(63) Boyarkin, O. V.; Mercier, S. R.; Kamariotis, A.; Rizzo, T. R. *J. Am. Chem. Soc.* **2006**, *128*, 2816.
(64) Mercier, S. R.; Boyarkin, O. V.; Kamariotis, A.; Guglielmi, M.; Tavernellim, I.; Cascella, M.; Rothlisberger, U.; Rizzo, T. R. *J. Am. Chem. Soc.* **2006**, *128*, 16938.

JP8091754